FINAL REPORT ON THE START PROGRAMME

MEASURING THE SPIN ALIGNMENT OF $K^*(892)^{\pm}$ MESONS IN THE SAND EXPERIMENT

Student: G. I. Vorobyev

                                                      Russia, MEPhI

Supervisor: Dr. Artem Chukanov

Participation period:

19.03.2023-13.05.2023

Dubna 2023

Table of contents:

1 Abstract

In this article we analyzed simulation data from **SAND** (System for on-Axis Neutrino Detection, the DUNE near detector) to investigate the presence of spin alignment in $K^*(892)^\pm$ resonances produced in neutrino charged current interactions.The obtained results demonstrated a uniform distribution of angles for the mesons, implying the absence of spin alignment and indicating that the spin of quarks has minimal influence on the process of fragmentation and hadronization. These findings are in line with the fact that the Monte Carlo data used in the analysis do not incorporate spin effects. The study's findings provide insights into quark behavior and strong force interactions, with potential applications for future particle physics research.

2 Introduction

Despite being abundant, neutrinos remain one of the most intriguing and least understood areas of particle physics. Their weak interaction with matter, described by the electroweak force, poses significant challenges in detecting and studying neutrinos. However, by studying neutrinos in greater detail, we can deepen our understanding of the fundamental nature of matter and the universe.

Neutrinos are important in astrophysics, as they are produced in large numbers by nuclear fusion in the sun and supernova explosions. Studying these neutrinos can provide new insights into the inner workings of stars and other astrophysical objects. Neutrinos play a crucial role in several unresolved puzzles in cosmology, including the matter-antimatter asymmetry in the universe and the enigma of dark matter. By studying neutrinos in more detail, we may be able to shed light on these mysteries.

In recent years, several neutrino experiments have provided significant progress in understanding neutrinos, such as the *T2K* experiment in Japan, which published new results that suggest a discrepancy between the behavior of neutrinos and antineutrinos. The *MINOS+* and *Daya Bay* experiments have also made precise measurements of the mixing angle that governs the oscillation of neutrinos between different flavors, confirming the previous measurements by other experiments. The *IceCube* experiment at the South Pole has detected a high-energy neutrino that appears to have originated outside of our galaxy, providing new insights into the sources and properties of these elusive particles.

Despite these advancements, new experiments are necessary to improve our understanding further. The upcoming **DUNE** (Deep Underground Neutrino Experiment) experiment [1; 2] aims to study neutrino properties and interactions by detecting charged current interactions in the near detector. **In this article**, we present the spin alignment measurement of $K^*(892)^{\pm}$ resonances produced by neutrinos in charged current interactions in the DUNE near detector and explore their impact on quark properties and fragmentation into hadrons. For this case we used Monte-Carlo simulated data since the experiment has not yet been started. The results may provide new insights into the behavior of quarks and the mechanisms of hadronization.

2.1 DUNE experiment

The Deep Underground Neutrino Experiment (DUNE) is a planned experiment set to take place at the end of the 2020s. It will study the oscillation of muon neutrinos into other types of neutrinos using a neutrino beam generated by the proton accelerator at the Fermilab laboratory. The Joint Institute for Nuclear Research and the laboratories associated with it are among the participants in this experiment, actively contributing to the development and refinement of technical and experimental methods.

The study of the neutrino beam will be conducted by two complex neutrino detectors, one located at Fermilab and the other at a far distance of 1300 km at the Sanford Laboratory.
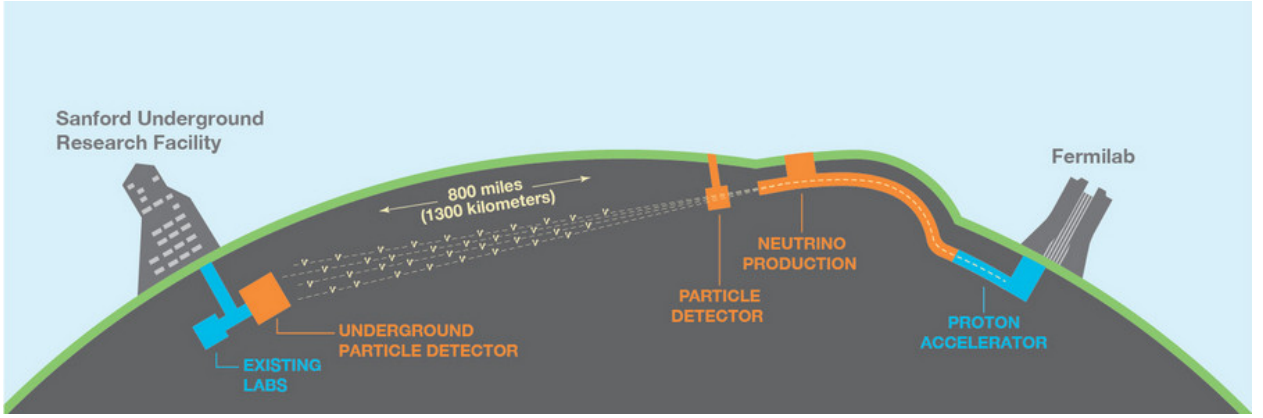
Figure 1: Neutrino production associated with DUNE

The objectives of the experiment are diverse, such as studying the mass hierarchy of the three neutrino states, exploring the mechanism by which neutrinos acquire mass, and searching for manifestations of violation of CP invariance.

One of the main advantages of the experiment Near Detector DUNE (SAND, see 2.3) is the anticipated number of recorded events, which will exceed $5.5 * 10^6$ charge current events per year. Although neutrinos are weakly interacting particles, advanced technical solutions and detector designs will allow for the detection of rare processes, making the number of events an order of magnitude higher than in previous experiments.

In summary, the DUNE experiment is a critical undertaking in our journey to comprehend the nature of the universe and the fundamental components of matter. It is expected to generate unprecedented data that will deepen our knowledge of neutrinos, shed light on unanswered physics questions, and propel us toward a more comprehensive understanding of the cosmos.
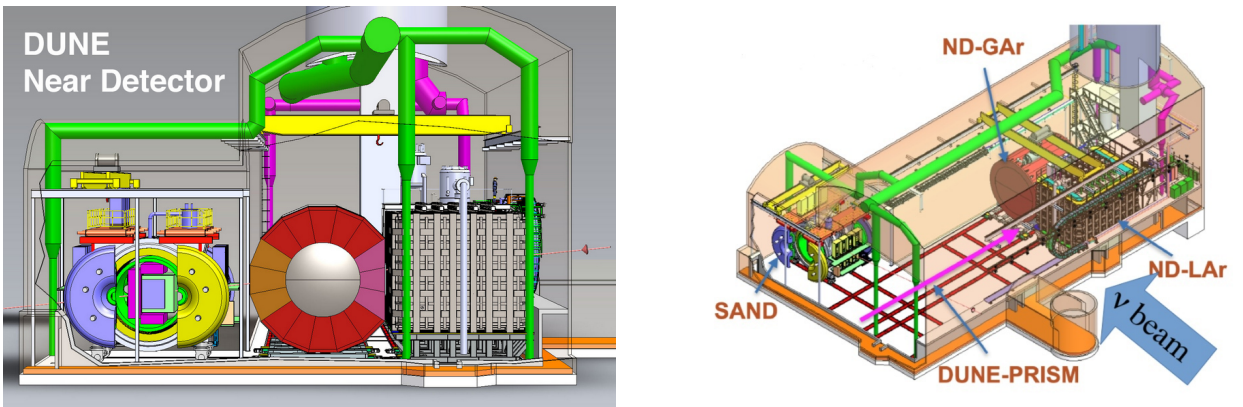
2.2   Near detector design

Figure 2: Near detector design

The DUNE near detector, which is a crucial component of the experiment, will be located at Fermilab, downstream of **LBNF** (Long-Baseline Neutrino Facility), and will be positioned approximately 600 meters away from the point of neutrino production [2]. The

near detector comprises of several sub-detectors that will be arranged side by side. Among these sub-detectors, **SAND** (the System for on-Axis Neutrino Detection) will be installed along the neutrino beam axis, while the other two sub-detectors, **NDLAr** (the Liquid Argon–based Near Detector for the DUNE experiment) and **NDGar** (the Gas Argon–based Near Detector for the DUNE experiment), will be movable and can be displaced in a direction perpendicular to the beam to detect neutrinos produced at various angles. With this configuration, the DUNE collaboration can accurately determine the composition of the neutrino beam without considering neutrino oscillations in the far detector at the Sanford Laboratory, located 1300 km away from Fermilab, in South Dakota. By accurately measuring the neutrino flux and energy spectrum at the near detector, scientists can better understand and reduce the uncertainties in the neutrino properties at the far detector, making the DUNE near detector a vital tool in the success of the overall experiment.

2.3   Detector SAND

The DUNE Near Detector system is composed of multiple detectors, including SAND, or the "on-axis" component, which will be located in a dedicated alcove downstream of the ND-LAr and ND-GAr detectors [2]. SAND is designed to reduce rescattering effects by using straw tubes in its inner tracker, allowing for more accurate measurements of the neutrino beam. Additionally, SAND has the capability to change the target material, such as hydrogen, to observe processes of particular interest (Fig.3).

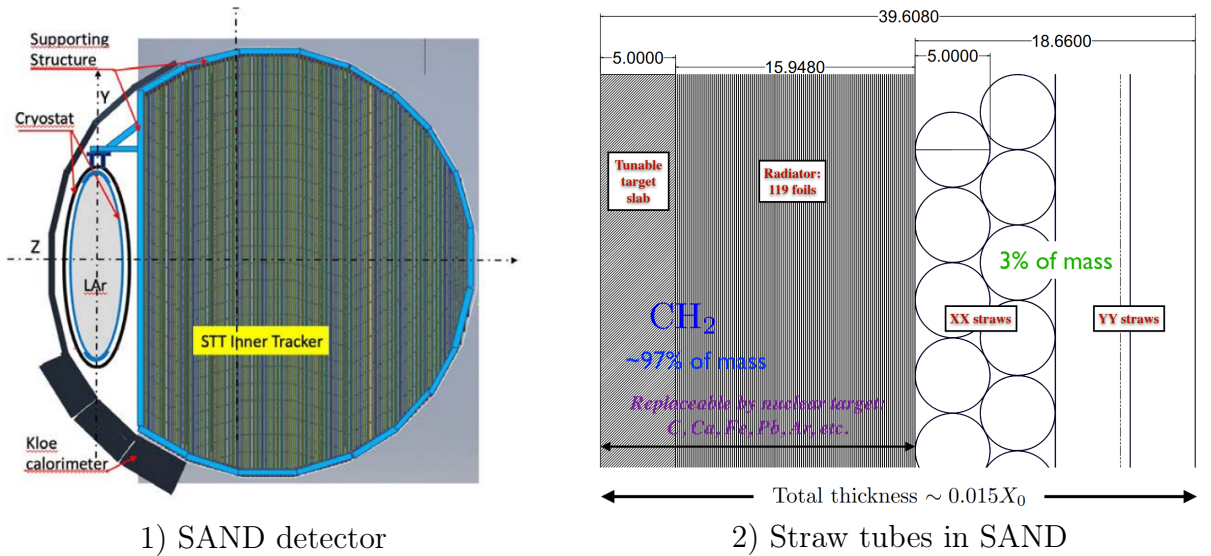1) SAND detector   2) Straw tubes in SAND

Figure 3: SAND detector construction

One of SAND's primary functions is to monitor the neutrino beam in real time and study any changes in beam parameters. The stationary nature of the detector also allows for a higher collection of statistics compared to the movable NDLAr and NDGar detectors. Another advantage of SAND is its ability to accurately detect individual tracks and calculate the cross section capability. Overall, the SAND detector plays a crucial role in the success

of the DUNE experiment by providing essential information about the properties of the neutrino beam.

3 Studies of $K^*(892)^{\pm}$ mesons

3.1 Invarian mass

The K^* meson and its decay products exhibit the same invariant mass, which refers to the mass of a particle in its rest frame. As a particle decays, information about it is lost, but the invariant mass can be determined from its decay products. Such method helps to confirm the production of K^* mesons. To calculate the squared invariant mass, denoted as M_{inv}^2, the sum of the squared energies of the decay products is subtracted from the sum of the squared momenta of the decay products. [3]:

$$M_{inv}^2 = (\sum_i E_i)^2 - ||\sum_i P_i||^2 \tag{1}$$

In our study, we utilize the ROOT software package to perform the invariant mass calculation procedure.

3.2 Event selection

The identification of K^* mesons involves a crucial step, which is the selection of events in which the meson was produced. First of all we focus on the following processes:

$$K^{*\pm} \to K^0 + \pi^{\pm}, \tag{2}$$

where K^0 refers to K^0_{short}, which further decays as:

$$K^0_{short} \to \pi^+ + \pi^-, \tag{3}$$

while excluding the decay mode:

$$K^0_{short} \to \pi^0 + \pi^0. \tag{4}$$

We choose to focus on the K^0_{short} decay because the *long* version of the K^0 has a longer lifetime, preventing its decay within our detector, thus making it undetectable. Although the decay $K^0_{short} \to \pi^0 + \pi^0$ can be measured with uncertainties due to triple reconstruction and product identification, for now, we only consider the charged decay of K^0_{short}. This selection allows us to proceed with the analysis while minimizing uncertainties in the invariant mass calculations.

Also we imposed a number of restrictions on the selected particles:

1. To prevent potential edge cases, a fiducial volume cut is applied as a selection criterion.

2. The presence of a muon in our event, since the muon is a well identified particle, then there is no need to introduce additional conditions for the reconstruction of the muon track when using the reconstruction program.

3. An important condition is that the K^0_{short} and $\pi^{\pm}$ particles tracks come out of the primary vertex. Within the framework of the experimental approach, this is determined by the fact that the distance from the event to the particle does not exceed 5 cm (in the future, this condition is subject to correction)

In the current study, we assume an identification efficiency of 100% for the pions and K-mesons.

3.3   Peak in particle events. Particle 2000000001

1) Invariant mass for $K^0 + \pi^+$ decay   2) Invariant mass for $K^0 + \pi^-$ decay
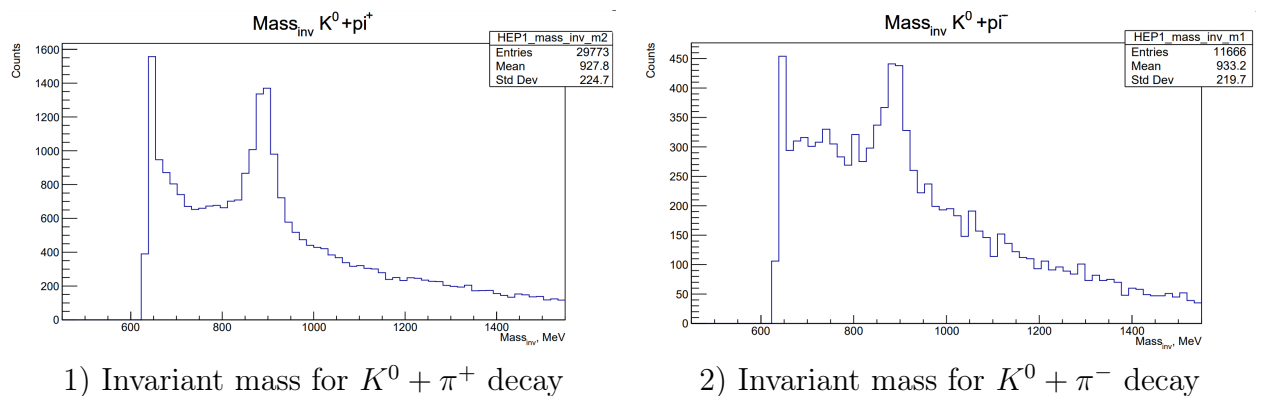
Figure 4: The histogram of invariant mass obtained from the selected events reveals an additional peak around 650 MeV that cannot be accounted for by existing theoretical explanations.

Based on the criteria described in section 3.2, we obtained a histogram of the invariant mass for $K^0 + \pi^{\pm}$ events. Unexpectedly, in this histogram, we observe a peak at 650 MeV (see Figure 4). Further experimental investigation revealed that events with common parents in primary vertex identified by PDG numbers 2000000001 (two billion and one) or 92 contribute to this peak. The PDG number 92 corresponds to a hadron string in classical explanation, while the nature of PDG number 2000000001 is still unknown. By selecting events only with PDG number 92 as parents, the invariant mass histogram exhibits a predictable shape without the observed peak. On the other hand, when considering events with parents having PDG number 2000000001 at the primary vertex, the presence of the peak in the invariant mass distribution becomes apparent.

The origin of this peculiar peak remains an open question, and it necessitates further investigation from the developers of the GENIE neutrino simulations program. For the current study, we will simply exclude events with PDG number 2000000001 at the primary vertex and focus on analyzing the remaining data to gain insights into the properties and behavior of the studied particles and fenomena.

3.4 Reconstructed data

1) Invariant mass for $K^0 + \pi^+$ decay
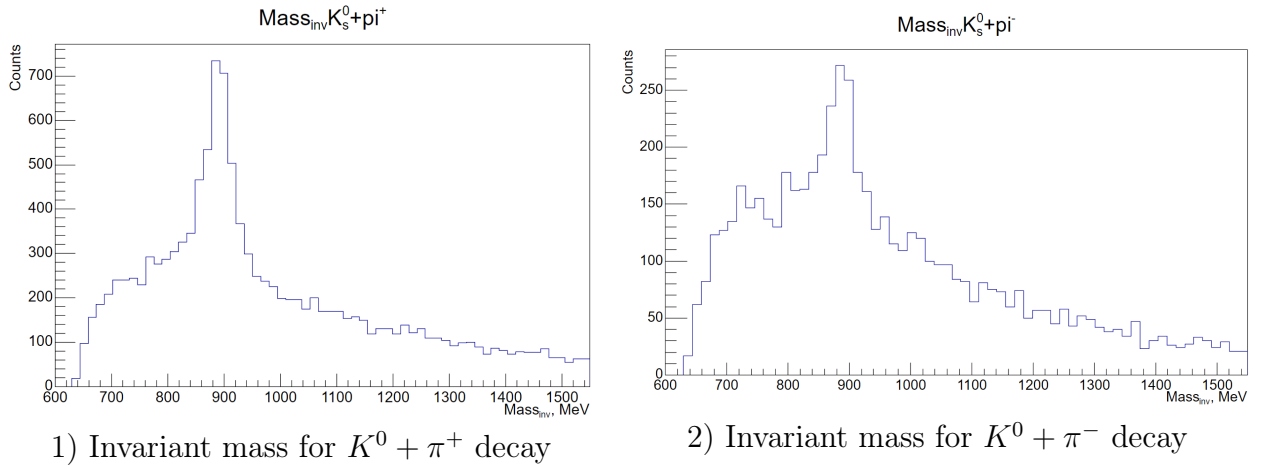
2) Invariant mass for $K^0 + \pi^-$ decay

Figure 5: The histogram of invariant mass obtained from «recostructed data» with event selection described in 3.2 and 2000000001 particle filter

The subsequent phase of the study involved the transition from Monte Carlo (MC) simulations to data reconstruction. It is essential to highlight that there is still no comprehensive reconstruction program in the conventional sense. Instead, we utilize «reconstructed data» that only include detectable particles. Consequently, particles such as neutral pions or K mesons, which are not directly observable, are excluded from the reconstructed data. However, we are able to observe the decay products of these particles.

To perform the reconstruction, we employ the invariant mass technique (see 3.1). By calculating the invariant mass, we reconstruct the four-momentum of the parent particle and numerically compare it with the four-momentum of similar particle types in the MC data. This comparison allows us to analyze the agreement between the reconstructed data and the MC simulations.

When we obtain the data and the invariant mass histogram (see fig. 5), we can perform a fitting analysis.

3.5 Signal fitting

In this work, a fitting analysis similar to the one described in the reference article [4] is performed. For the background component, a polynomial function is employed.

$$BG = a_1 \Delta^{a_2} e^{-(a_3 \Delta + a_4 \Delta^2)} \tag{5}$$

where $\Delta = M_{\mathrm{res}} - M_{\mathrm{min}}$, M_{res} is the invariant mass of the pair $K0 + \pi$, M_{min} — the minimum value of the invariant mass (at rest)

For signal we use fucntion decribed in ROOT framework [5]:

$$\mathrm{TMath::BreitWigner} = \frac{1}{2\pi} \cdot \frac{\Gamma}{(M_{\mathrm{res}} - M_0)^2 + (\Gamma/2)^2}, \tag{6}$$

8

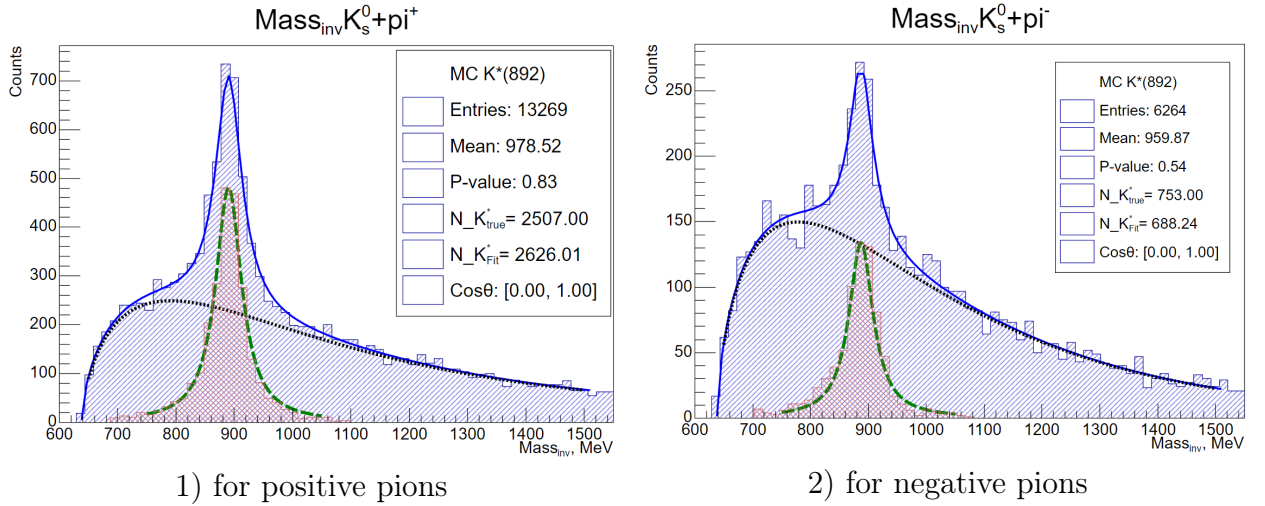|	
1) for positive pions	2) for negative pions

Figure 6: Fitted histogram for invariant mass of $K^0 + \pi$. Line description: *Blue solid line* — total (background + signal) fit; *the green dashed line* is the real $K^*(892)$ fit (signal fit = combinatorial mass - background); *black dotted line* - background fit; *filled red histogram* - real $K^*(892)$ (signal from MC data); *blue filled histogram* - MC data of combinatorial invariant mass

Table 1: Numerical characteristics in the process with $K^{*\pm}$

Meaning	Symbol	Value
Number of simulated ν_μ cc processes	N_ν^{sim}	2064693
Number of reconstructed ν_μ cc processes	N_ν^{rec}	2063976
Neutrino reconstruction efficiency	$\varepsilon_\nu = N_\nu^{rec}/N_\nu^{sim}$	0,99965
Number of reconstructed $K^0 \to \pi^- \pi^+$ events	$N_{K^0 \to \pi^- \pi^+}^{rec}$	10456

where Γ — decay width, M_0 — peak value of resonance.

The final plots are presented in Figure 6. The legend accompanying the plots provides information about the quality characteristics of the fit, such as the P-value. The P-value is calculated using the inner methodology of ROOT based on the χ^2 criterion. Additionally, we provide the number of $K^*(892)^\pm$ mesons obtained from the selected events. This value is calculated from the integral of the signal fit (N_K$^*_{\text{fit}}$) and from the integral of the «true» $K^*(892)^\pm$ histogram (N_K$^*_{\text{True}}$). The «true» histogram, filled with red, is obtained from the MC data, where all particles are visible. This histogram serves as a visual check for the analysis.

3.6 Identification efficiency of K^{*0}

To complete our analysis, we decided to find the efficiency value and the relative number of outputs for $K^{*\pm}$ decayed into $K^0\pi^\pm$ pairs, intermediate values are presented in tables 1, 2.

Table 2: Event reconstruction efficiencies

Meaning	Symbol	K^{*+}	K^{*-}
Number of simulated $K^*(892)$ events	$N_{K^*}^{sim}$	9519	2855
Number of reconstructed $K^*(892)$ events	$N_{K^*}^{rec}$	2702	824
Number of identified from fit $K^*(892)$ events	$N_{K^*}^{fit}$	2806	779
Relative number of reconstructed K^* to $K^0 \to \pi^- \pi^+$ events	$N_{K^*}^{rec}/N_{K^0 \to \pi^- \pi^+}^{rec}$	0.26	0.08
In process $K^* \to K^0 \pi^\pm, K^0 \to \pi^- \pi^+$:			
Efficiency of reconstruction	$\varepsilon = N_{K^*}^{rec}/N_{K^*}^{sim}$	0.28	0.29
Yields, %	$P = N_{K^*}^{sim}/N_\nu^{sim}$	0.46	0.14
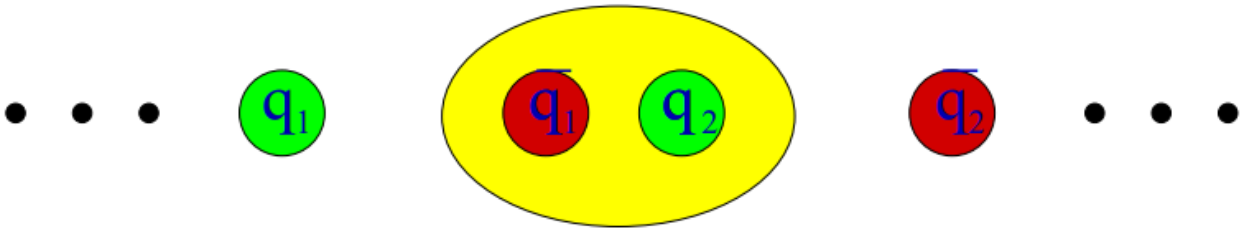
Figure 7: Meson production in the process of string fragmentation

4 Studies of Spin Aligment

4.1 Theory

The string model is a phenomenological framework used to study hadronization, providing a simplified and useful mechanism to investigate the spin of forming quarks. According to this model, a quark-antiquark pair forms a string-like configuration. In high-energy collisions, if there is sufficient string tension, the string can break into three pieces, with the original quark and two new quarks. The spins of all these quarks are expected to be correlated [4].

In our study, we focus on the production of mesons and examine the spin correlation between the forming quarks and the resulting mesons. The forming quarks can have four possible spin configurations: ↑↑, ↑↓, ↓↑, and ↓↓. These spin configurations can lead to the production of mesons such as:

$$|1,1\rangle = |++\rangle,$$
$$|1,0\rangle = \frac{1}{\sqrt{2}}(|+-\rangle + |-+\rangle),$$
$$|0,0\rangle = \frac{1}{\sqrt{2}}(|+-\rangle - |-+\rangle),$$
$$|1,-1\rangle = |--\rangle \tag{7}$$

We have vector mesons (states with spin 1 and 3 possible projections) and pseu-

doscalar mesons (state with spin 0, represented by $|0,0\rangle$). If all these states have equal probabilities, the probability of producing a pseudoscalar meson (P) compared to a vector meson (V) is given by $P/V = 1/3$.

However, if these states do not have equal probabilities, taking into account the correlation of quarks ($P_{q\bar{q}}$), the ratio of P to V becomes:

$$\frac{P}{V} = \frac{1 - P_{q\bar{q}}}{3 + P_{q\bar{q}}}, \tag{8}$$

This ratio of P to V approximately equal to the diagonal element of the spin density matrix, ρ_{00}. The angular distribution of vector mesons decay products can be described by equation:

$$W(\cos\theta) = \frac{3}{4}[(1 - \rho_{00}) + (3\rho_{00} - 1)\cos^2\theta], \tag{9}$$

where W represents the angular distribution and θ is the angle between the direction of one of the outgoing products in the rest frame and the direction of the vector meson (parent, z-axis).

By analyzing this angular distribution, we can determine the value of ρ_{00} and infer the presence or absence of spin alignment or correlation ($P_{q\bar{q}} = 0$). Specifically:

1. $\rho_{00} = 1/3 \Rightarrow W = 1/2$. no spin alignment; the probability of projections +1, -1 and 0 of the meson spin onto the z axis are equal (in this case there is no dependence of equation on $\cos\theta$));

2. $\rho_{00} = 0$. spin alignment; only the +1 and -1 projections are possible;

3. $\rho_{00} = -1$. spin alignment; only the 0 projection is possible.

By studying the angular distribution of $K^0 + \pi$ in data, we can explore the relationship between P and V and determine if there is any spin correlation or if $P_{q\bar{q}} = 0$.

4.2   Results

In our analysis, we divided the events into five different ranges of angles and determined the number of K* mesons within each range. This number was obtained using a similar method as described in Section 3.5.

We observed the presence of a slope in the data, as shown in Figure 8. This slope indicates that a correction will be necessary for the real data based on this observed trend. Additionally, using the standard fitting tools provided by the ROOT framework, we obtained the parameter ρ_{00}, results shown in 10.

$$\rho^{\pi+} = 0.302 \pm 0.016$$
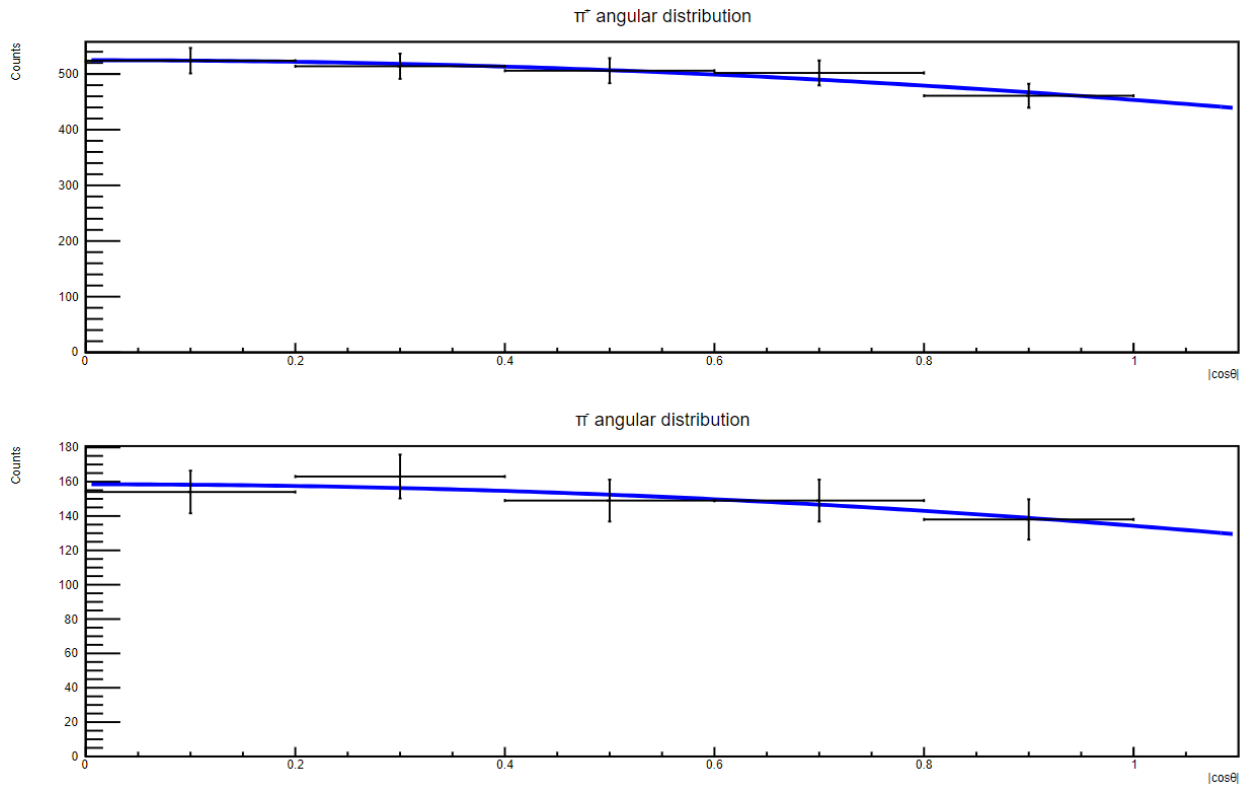$$\rho^{\pi-} = 0.298 \pm 0.028 \tag{10}$$

11

Figure 8: Angular distribution for $K^0 + \pi$. On x-axis we use absolute meaning of $\cos\theta$
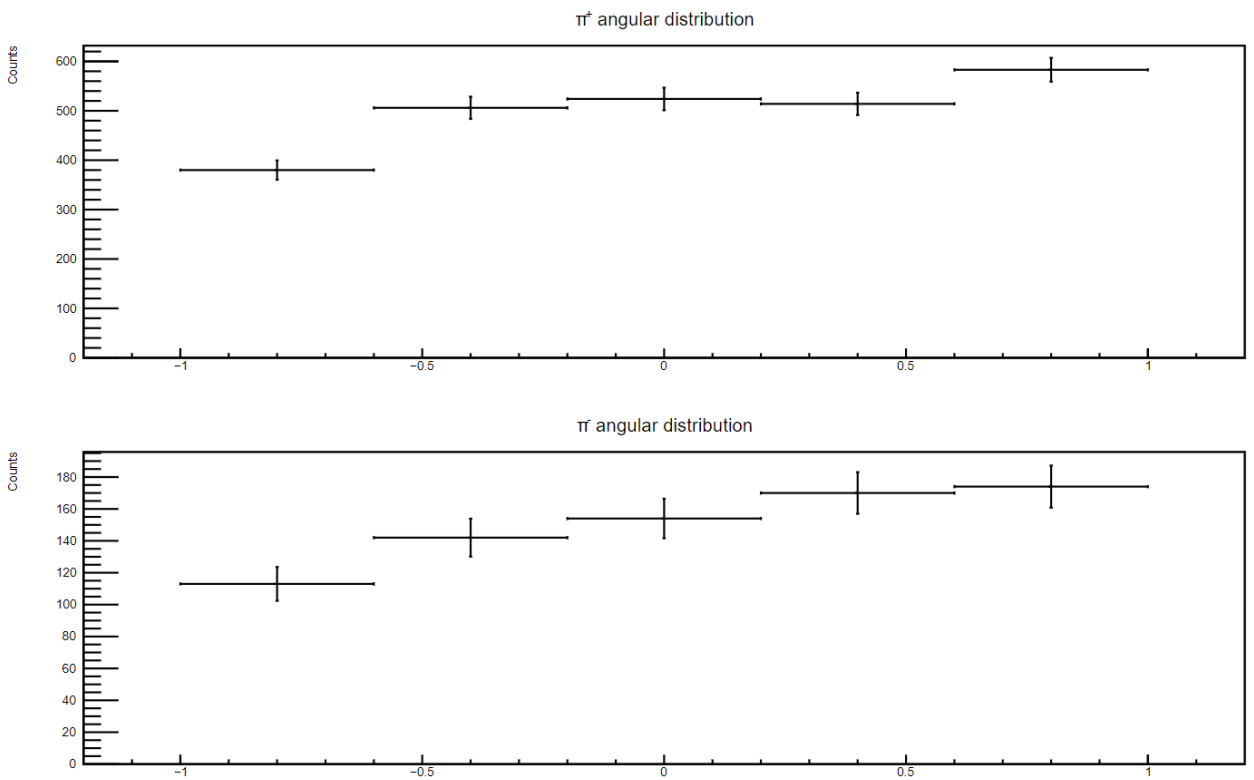

Figure 9: Angular distribution for $K^0 + \pi$.

To further understand the nature of this slope, we examined the cosine distribution without absolute values, as shown in Figure 9. We noticed a lack of events where the pions were emitted in the opposite direction to the K* mesons. This suggests that the reconstruction efficiency for these particular pions is significantly lower compared to those emitted in the same direction as the K* mesons. A possible explanation for the lack of events with pions emitted in the opposite direction to the K* mesons is that these pions may have very low momenta. As a result, their trajectories could be relatively small, making it challenging for them to be detected by the experimental setup.

5 Conclusion

In this work, we studied the vector K* meson in simulated SAND data.

- During the course of our research, we conducted an analysis of the event selection process, obtained histograms of the distributions of invariant masses for the decay of samples into charged tracks, and performed a fit.

- Based on the results of the fit, we measured the number of produced K*(892) mesons.

- We also measured the alignment of spins for the selected events. From the angular distribution, we obtained values of the parameter ρ_{00}. The obtained results correspond to unaligned spins.

For future tasks we can define:

1. Repeat analysis for lambda hyperons

2. Understand the reason for the appearance of the peak for 750 MeV π^- (write to the authors of Genie)

3. Measure the yields of strange baryon resonances $\Sigma^{*\pm}$ and baryon Ξ^- , to tune the simulation program

6 Acknowledgment

References

1. *DUNE collaboration.* James Strait(Fermilab) for the collaboration. —.

2. *DUNE collaboration.* Deep Underground Neutrino Experiment (DUNE) Near Detector Conceptual Design Report. — ; — https://arxiv.org/abs/2103.13910.

3. *L.D. Landau, E.M. Lifshitz.* The Classical Theory of Fields: 4th revised English Edition: Course of Theoretical Physics // Vol. 2. Butterworth Heinemann. — 1975.

4. *Chukanov A.* Production properties of $K^*(892)^{\pm}$ vector mesons and their spin alignment as measured in the NOMAD experiment // NOMAD Collaboration. — 2006. — https://arxiv.org/pdf/hep-ex/0604050v1.pdf.

5. *Brun R., Kreshuk A., et. al.* TMath: Encapsulate math routines. — ROOT, 2009. — https://root.cern.ch/root/html524/src/TMath.cxx.html#ADLSVE.